

JET STRUCTURE STUDIES AT LEP AND HERA<sup>†</sup>

J. WILLIAM GARY

*Department of Physics, University of California, Riverside CA 92521, USA**E-mail: bill.gary@ucr.edu*

A summary of some recent studies in jet physics is given. Topics include leading particle production in light flavor events in  $e^+e^-$  annihilations, an analytical treatment of gluon and quark jets at the next-to-next-to-next-to-leading order (3NLO), and various studies performed at LEP and HERA involving separated gluon and quark jets.

### 1 Leading particle production in separated light quark events

Separated charm (c) and bottom (b) quark events have been well studied in  $e^+e^-$  annihilations. c and b quarks are mostly produced at the electro-weak vertex in  $e^+e^- \rightarrow q\bar{q} \rightarrow \text{hadrons}$  events, in which the primary quark q is c or b, and are relatively easy to identify. In contrast, separated up (u), down (d) and strange (s) events have not been much studied. u, d and s quarks are copiously produced during jet development, making events in which they are produced as primary quarks more difficult to identify.

A recent study<sup>1</sup> by the OPAL Collaboration at LEP identifies  $e^+e^- \rightarrow q\bar{q} \rightarrow \text{hadrons}$  events with  $q=u, d$  or  $s$ . The probabilities  $\eta_q^i(x_p^{min.})$  are determined for the quark  $q=u, d, s$  (or charge conjugate) to appear in an identified hadron  $h_i(x_p^{min.})$ , where  $h_i=\pi^+, K^+, K_S^0, p$ =proton, or  $\Lambda$  (or charge conjugate) is the leading particle in the jet, i.e. it has the largest momentum, with a scaled momentum  $x_p=2p/\sqrt{s}$  larger than a minimum  $x_p > x_p^{min.}$ , where  $\sqrt{s}=91$  GeV. The  $\eta_q^i$  probabilities provide unique, detailed information on the hadronization process and a more di-

rect determination of basic hadronization parameters such as the strange quark suppression factor  $\gamma_s \equiv \text{Prob.}(s)/\text{Prob.}(u \text{ or } d)$  than in most previous studies.

The method for the measurement is presented in ref.<sup>2</sup>. Briefly,  $e^+e^- \rightarrow \text{hadrons}$  events are divided into hemispheres using the plane perpendicular to the thrust axis. Thus an *inclusive* definition of jets is used, i.e. a jet is an event hemisphere. The single and double tag rates in the jets are measured,  $N_i(x_p^{min.})/N_{had.}$  and  $N_{ij}(x_p^{min.})/N_{had.}$ , where  $N_i(x_p^{min.})$  is the number of jets in which the highest momentum particle has  $x_p > x_p^{min.}$  and is identified as  $\pi^+, K^+, K_S^0, p$  or  $\Lambda$ , and  $N_{ij}(x_p^{min.})$  is the analogous quantity for events in which a hadron  $h_i$  is identified in one hemisphere and hadron  $h_j$  is identified in the other.

$$\begin{aligned} \frac{N_i(x_p^{min.})}{N_{had.}} &= 2 \sum_{q=u,d,s,c,b} \eta_q^i(x_p^{min.}) R_q \\ \frac{N_{ij}(x_p^{min.})}{N_{had.}} &= (2 - \delta_{ij}) \times \\ &\sum_{q=u,d,s,c,b} \rho_{ij}(x_p^{min.}) \eta_q^i(x_p^{min.}) \eta_q^j(x_p^{min.}) R_q \end{aligned}$$

is then solved, where  $R_q = \frac{\Gamma_{Z^0 \rightarrow q\bar{q}}}{\Gamma_{Z^0 \rightarrow \text{hadrons}}}$  is the partial decay width of the  $Z^0$  to the different quark flavors, taken from the standard model for  $q=u, d, s$  and from LEP for  $q=c, b$ , and  $\rho_{ij}$  are hemisphere correlations due mostly

<sup>†</sup>Talk presented at the XXXth International Conference on High Energy Physics, July 27 - August 2, 2000, Osaka, Japan.

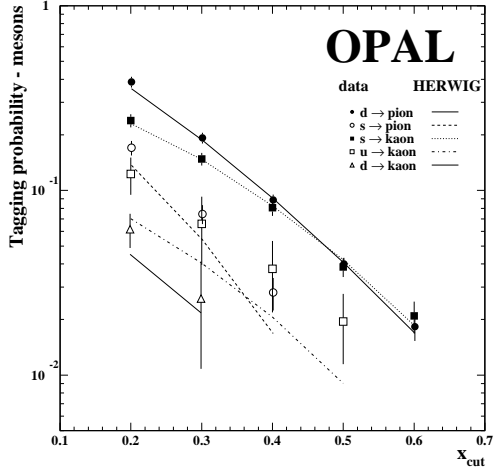


Figure 1. Tagging probabilities for pions and kaons as a function of the minimum scaled momentum  $x_p^{min}$ , in comparison to Monte Carlo predictions.

to well understood effects such as geometric acceptance and gluon bremsstrahlung. The  $\rho_{ij}$  factors are evaluated using QCD Monte Carlo and are the only MC information entering the equations. Their values are typically  $\rho_{ij} \approx 1.01$ -1.10. To solve the above system of equations, supplementary information involving assumptions of isospin symmetry and the flavor independence of the strong interaction are invoked (see refs.<sup>1,2</sup>).

The measured probabilities  $\eta_q^i$  for  $i=\pi$  and  $K$  are shown in figure 1 as a function of  $x_p^{min}$ . From this figure, the so-called leading particle effect is clearly visible, i.e. primary quarks appear primarily as valence quarks in the highest momentum hadrons. Thus d and u quarks appear predominantly in pions, and s quarks in kaons, rather than vice versa. The leading particle effect has been observed many times for b and c quarks. There is only one previous study of the effect for light quarks, given in ref.<sup>3</sup>.

Using the probabilities  $\eta_q^i$ , basic hadronization parameters such as the strange quark suppression factor  $\gamma_s$  can be determined

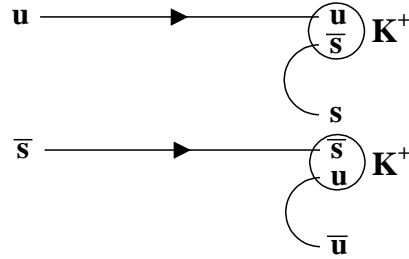


Figure 2. Illustration of the determination of the strangeness suppression factor  $\gamma_s$  from the ratio of the tagging probabilities for  $K^\pm$  mesons to be produced either from a primary u quark (top) or primary  $\bar{s}$  quark (bottom).

rather directly. For example the probability factors  $\eta_u^{K^\pm}$  and  $\eta_s^{K^\pm}$  differ only by  $s\bar{s}$  or  $u\bar{u}$  pair production from the sea, see figure 2. Their ratio thus determines  $\gamma_s$ . Note that most other measurements of  $\gamma_s$  either compare the yields of hadrons with different masses, such as kaons and pions, or else rely on the tuning of Monte Carlo parameters. They are thus not as direct as the method described here which employs kaons only. The result for  $\gamma_s$  is  $0.422 \pm 0.049$  (stat.)  $\pm 0.059$  (syst.), about one standard deviation higher than the result in ref.<sup>3</sup> based on a similar technique.

## 2 Experimental properties of gluon and quark jets from a point source

The inclusive (hemisphere) definition of jets yields unbiased jets whose properties can be compared directly to the predictions of analytic calculations. Inclusive production of hadrons in  $e^+e^-$  annihilations provides a natural source for unbiased quark jets, used – for example – in the study described in section 1. One can ask if an analogous sample of high energy unbiased gluon jets can be identified.

The answer, as discussed in ref.<sup>4</sup>, is yes, by selecting rare events in  $e^+e^-$  annihilations in which two identified quark jets appear in the same hemisphere of an event. The oppo-

site hemisphere, against which the two quark jets recoil, approximates an unbiased gluon jet with high accuracy<sup>4</sup>. Such events have been labeled  $e^+e^- \rightarrow q_{\text{tag}}\bar{q}_{\text{tag}}g_{\text{incl.}}$  events to differentiate them from “ordinary”  $q\bar{q}g$  three-jet events defined using a jet finder. The tagged quark jets  $q_{\text{tag}}$  and  $\bar{q}_{\text{tag}}$  are identified using b tagging. The recoiling hemisphere “ $g_{\text{incl.}}$ ” is the unbiased gluon jet.

Experimental analysis of  $g_{\text{incl.}}$  jets from  $Z^0$  decays has been presented by OPAL<sup>5</sup>. Starting from their full LEP-1 data sample of about 4 million events, a sample of 439  $g_{\text{incl.}}$  jets is isolated with a purity of about 82%. The  $g_{\text{incl.}}$  jet energy is about 40 GeV. The  $g_{\text{incl.}}$  jets are compared to a sample of light (u,d and s) quark jets, also from  $Z^0$  decays, defined using the hemisphere definition. The quark jet sample is restricted to light flavors to better approximate the massless quark condition employed by analytic calculations.

Only one aspect of the results will be presented here, namely the ratio of soft particles at large transverse momentum  $p_{\perp}$  between the unbiased gluon and quark jets.  $p_{\perp}$  is defined with respect to the jet axis. As discussed in ref.<sup>6</sup>, this ratio provides a direct measurement of the QCD color factor ratio  $C_A/C_F$ .

Figure 3 shows the charged particle multiplicity ratio between the unbiased gluon and quark jets,  $r$ , as a function of the softness of the particles. The softness of the particles is defined by the maximum particle momentum  $p_{\text{max.}}$  considered when determining  $r$ . The particles are required to have  $p_{\perp} > 0.8$  GeV/c. Particles with  $p_{\perp} < 0.8$  GeV/c are dominated by the effects of hadronization as is established using MC. The solid curve shows the prediction of the Herwig Monte Carlo.

With no explicit cut on  $p_{\text{max.}}$  (“All momenta”) the multiplicity ratio is predicted to be about 1.8. As softer and softer particles are selected ( $p_{\text{max.}}$  is decreased), the curve approaches the QCD result  $C_A/C_F=2.25$  as

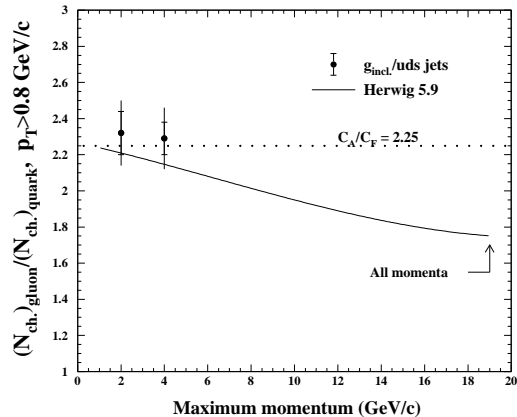


Figure 3. Ratio  $r$  of charged particle multiplicities between unbiased gluon and quark jets for particles with large transverse momenta to the jet axis defined by  $p_{\perp} > 0.8$  GeV/c. The results are shown as a function of the softness of the particles, defined by the maximum particle momentum used to determine  $r$ .

predicted in ref.<sup>6</sup>. OPAL results are shown for  $p_{\text{max.}}=2$  GeV/c and 4 GeV/c. The result using  $p_{\text{max.}}=4$  GeV/c is  $r=2.29 \pm 0.017$  (stat. + syst.) which provides one of the most accurate current experimental determinations of  $C_A/C_F$ . Note that unlike *all other methods*, this result is not based on a fit of a QCD motivated expression – in which  $C_A/C_F$  is extracted as a fitted parameter – but is the ratio of directly measured quantities.

### 3 Analytic description of multiplicity in gluon and quark jets

An analytic description of multiplicity in unbiased gluon and quark jets has recently been performed at the next-to-next-to-next-to-leading order (3NLO) in perturbation theory<sup>7</sup>. Details of the calculation are presented in refs.<sup>7,8</sup>. Here some comparisons of the results with experiment will be discussed.

The currently available measurements of mean multiplicity in unbiased gluon jets,  $n_G$ , from the CLEO Collaboration at CESR<sup>9</sup> at low energies and from OPAL  $g_{\text{incl.}}$  jets<sup>5</sup> at high energy, are shown in figure 4. The

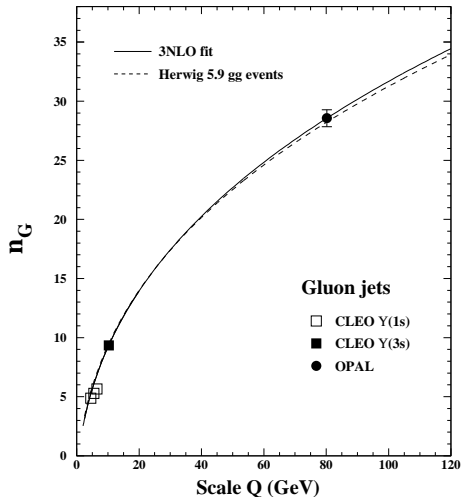


Figure 4. Measurements of unbiased gluon jet charged particle multiplicity in comparison to Monte Carlo and the 3NLO analytic predictions.

dashed curve is the prediction of Herwig, which describes the data rather well. The solid curve is a fit of the 3NLO analytic prediction<sup>7</sup> using two free parameters: (1) an overall normalization  $K$  and (2) an effective QCD scale parameter  $\Lambda$ . Translating the fitted result for  $\Lambda$  into  $\alpha_S(M_Z)$  yields  $\alpha_S(M_Z) = 0.14 \pm 0.01$ , not too different from the world average value  $\alpha_S(M_Z) \approx 0.12$  found using  $\Lambda_{\overline{MS}}$ .

Measurements of mean multiplicity in unbiased quark jets,  $n_F$ , performed by many experiments, are shown in figure 5. Again Herwig (dashed curve) describes the data rather well. Making a one parameter fit of the 3NLO expression for quark jet multiplicity<sup>7</sup> to the data (solid curve), with  $\Lambda$  as the fitted parameter and with the normalization  $K$  fixed from the fit to the gluon jet data, yields  $\alpha_S(M_Z) = 0.135 \pm 0.002$ , not very different from the result presented above for gluon jets. This demonstrates the consistency of the analytic approach to the growth of multiplicity with scale. Note that the inclusive (unbiased) definition of jets is crucial to obtain this result. If the quark and gluon jets are defined using a jet finder such as the  $k_{\perp}$

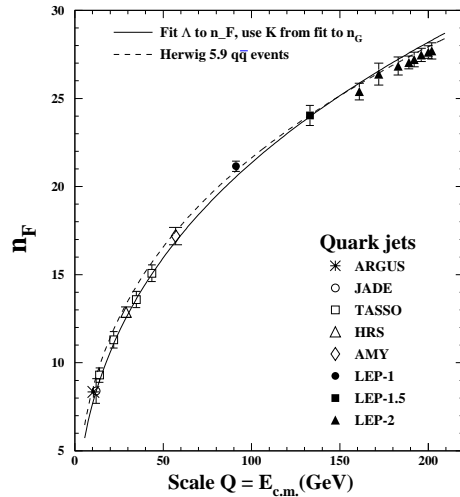


Figure 5. Measurements of unbiased quark jet charged particle multiplicity in comparison to Monte Carlo and the 3NLO analytic predictions.

jet finder, such consistency is not observed (see ref.<sup>7</sup>).

One other result will be discussed here, namely the ratio of the *slopes* of multiplicity, defined by  $r^{(1)} = \frac{d\langle n_G \rangle / dy}{d\langle n_F \rangle / dy}$  where  $y = \ln(Q/\Lambda)$  with  $Q$  the jet energy. The ratio of slopes  $r^{(1)}$  has the same asymptotic limit of 2.25 as  $r$ , but is predicted<sup>7</sup> to have smaller pre-asymptotic corrections. The 3NLO prediction for  $r^{(1)}$  versus  $Q$  is shown in figure 6 in comparison to measurements from OPAL<sup>10</sup> and the DELPHI<sup>11</sup> Collaboration at LEP. The experimental results exhibit some scatter because of differences in the definition of jets but are in general agreement with the prediction  $r^{(1)} \approx 1.9$ .

#### 4 Substructure dependence of dijet cross sections in photoproduction at HERA

A recent study from the ZEUS Collaboration at HERA concerns the photoproduction of dijets in low  $Q^2$  ep scattering<sup>12</sup>. Specifically, the reaction  $\gamma p \rightarrow 2 jets + X$  is studied, where the two-jet system is either  $q\bar{q}$ , gg

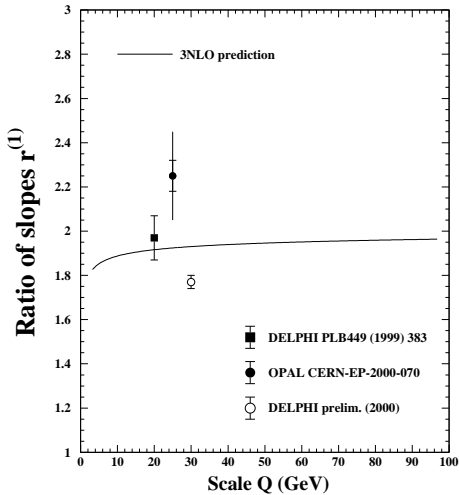


Figure 6. The ratio of slopes  $r^{(1)}$  between gluon and quark jets in comparison to the 3NLO analytic prediction.

or  $qg$ . Jet shapes (see below) are used to tag samples enhanced in quark and gluon jets. Measurements are then made of the rapidity distributions of the jets.

Events with at least two jets are selected using the longitudinally invariant  $k_{\perp}$  jet finder. Events are retained if they contain at least two jets with transverse energy  $E_T > 14$  GeV in the pseudo-rapidity range  $-1 < \eta < 2.5$ , where  $\eta = -\ln(\tan(\theta/2))$ , with  $\theta$  the polar angle with respect to the proton beam direction. The two jets with highest  $E_T$  are analyzed. Specifically, the jet profiles and sub-jet multiplicities of these jets are determined. The jet profile  $\Psi(r)$  is the distribution of the fraction of jet energy inside a cone of half radius  $r$  around the jet axis, relative to a cone with  $r=1$  radians.

The mean profile of the selected jets is presented in figure 7. The data, shown by the points, are well represented by the Monte Carlo, indicated by the solid line. The individual contributions of gluon and quark jets as predicted by the simulation are shown by the dashed and dash-dotted curves, respectively. The profiles of the gluon and quark jets are seen to differ substantially. In par-

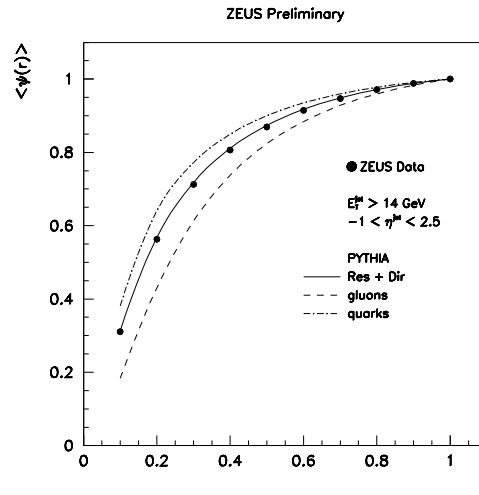


Figure 7. Jet profile of the two highest energy jets in  $\gamma p \rightarrow 2 jets + X$  events.

ticular, gluon jets are predicted to be much less collimated around the jet axis than quark jets, a fact that has been well established experimentally in  $e^+e^-$  collisions<sup>13</sup>.

Choosing a cone size  $r=0.3$  radians, quark and gluon jet dominated samples are selected by requiring  $\Psi(r=0.3) > 0.8$  or  $\Psi(r=0.3) < 0.6$ , respectively. The resulting samples are denoted “thin” jets and “thick” jets and have quark and gluon jet purities of about 85% and 60%, again respectively. The rapidity distributions of “thin” and “thick” jets are shown in figure 8 by the open and solid points. The curves show the Monte Carlo predictions for quark and gluon jets in  $\gamma p$  collisions. Gluon jets are produced mostly through *resolved* processes, in which the photon in the  $\gamma p$  collision acts as a source of partons. In contrast, quark jets are produced mostly through *direct* processes in which the photon couples directly to partons in the proton. This explains the different rapidity distributions predicted for gluon and quark jets. The “thick” and “thin” jet measurements are seen to follow the predictions for gluon and quark jets quite well, demonstrating a successful separation and test of the cross sections for gluon and quark jets individually.

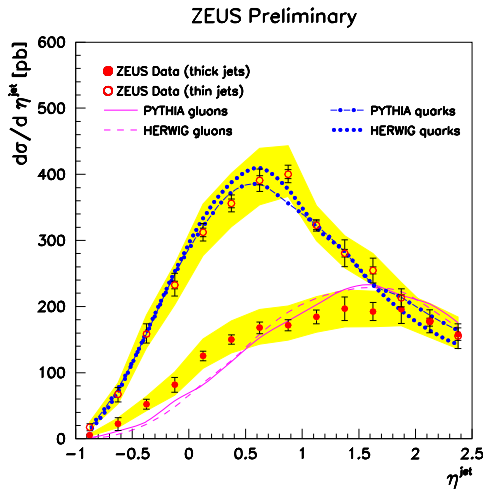


Figure 8. Rapidity distribution of “thick” and “thin” jets in comparison to the Monte Carlo predictions for gluon and quark jets in  $\gamma p$  collisions.

## 5 $\pi^0$ , $\eta$ , $K^0$ and charged particle multiplicities in quark and gluon jets

Last, I discuss a recent study from OPAL<sup>10</sup> on differences in the production rates of identified particles in gluon and quark jets.

QCD predicts that  $r_h$  – the ratio of the mean multiplicities of identified hadrons between gluon and quark jets – is the same for all hadrons  $h$ . In practice,  $r_h$  might differ for different particles because of the decay properties of hadrons or because of dynamical differences between the hadronization of gluons and quarks. For example, the gluon octet model of Peterson and Walsh<sup>14</sup> predicts  $r_h$  to be larger for isoscalar particles than for non-isoscalars, e.g. an enhancement in  $r_h$  for  $\eta$  mesons compared to charged particles. So far, studies at LEP of identified particles in gluon jets have either considered (1)  $\pi^+$ ,  $K^+$ ,  $p$ ,  $K_S^0$  and  $\Lambda$  production (or c.c.) in identified samples of gluon and quark jets<sup>15</sup>, leading to experimental determinations of  $r_h$ , or else (2) the production of  $\pi^0$ ,  $\eta$ ,  $\eta'$ ,  $K_S^0$  and  $\Lambda$  (or c.c.) in the lowest energy jet of  $e^+e^-$  three-jet events in comparison to the correspond-

ing result for charged particles or to Monte Carlo predictions<sup>16,17,18</sup>. The OPAL study discussed here is the first to employ the former strategy for  $\pi^0$  and  $\eta$  mesons, i.e. the first to determine  $r_h$  for  $\pi^0$  and  $\eta$ .

Three-jet events are selected using the  $k_\perp$ , cone, or LUCCLUS jet finders: the difference in the results defines a systematic uncertainty related to the jet definition. The jets are ordered such that jet 1 has the highest energy and jet 3 the lowest. The jet energy specifies the gluon jet content of the jet. The jets are then examined in terms of the so-called hardness scale<sup>19</sup>  $Q_{\text{jet}} = E_{\text{jet}} \sin(\theta_{\text{min.}}/2)$ , where  $\theta_{\text{min.}}$  is the smaller of the angles with respect to the two other jets. The hardness scale has been shown<sup>11</sup> to be a much more appropriate scale than the jet energy  $E_{\text{jet}}$  when comparing jets embedded in a three-jet environment, i.e. when comparing biased jets, as opposed to the unbiased jets discussed in sections 1-3.

The  $\pi^0$ ,  $\eta$ ,  $K_S^0$  and charged particle rates in jets 2 and 3 are compared in their overlap region, defined by  $7 < Q_{\text{jet}} < 30$  GeV. The multiplicity measurements are unfolded algebraically using the known quark and gluon jet content of jets 2 and 3 to obtain results corresponding to pure gluon and quark jets. The results for  $r_h$  for  $\pi^0$ ,  $\eta$  and  $K_S^0$  are then divided by the corresponding result for charged particles to obtain:

$$\begin{aligned} r_\eta/r_{ch.} &= 1.09 \pm 0.12 \\ r_{\pi^0}/r_{ch.} &= 1.01 \pm 0.04 \\ r_{K_S^0}/r_{ch.} &= 0.95 \pm 0.04 \end{aligned}$$

All three results are consistent with unity, indicating no evidence for a dynamical difference in the hadronization of gluon and quark jets. This conclusion is in agreement with recent results from the ALEPH Collaboration at LEP<sup>18</sup>. The OPAL and ALEPH results for  $\eta$  mesons contradict the conclusion of an earlier study<sup>17</sup> by the L3 Collaboration at LEP, in which evidence for a dynamical enhancement of  $\eta$  mesons in gluon jets was reported.

## References

1. OPAL Collab., G. Abbiendi et al., CERN-EP/99-164.
2. J. Letts and P. Mättig, *Z. Phys. C* **73**, 217 (1997).
3. SLD Collab., K. Abe et al., *Phys. Rev. Lett.* **78**, 3442 (1997).
4. J.W. Gary, *Phys. Rev. D* **49**, 4503 (1994).
5. OPAL Collab., G. Alexander et al., *Phys. Lett. B* **388**, 659 (1996); OPAL Collab., K. Ackerstaff et al., *Eur. Phys. J. C* **1**, 479 (1998); OPAL Collab., G. Abbiendi et al., *Eur. Phys. J. C* **11**, 217 (1999).
6. V. Khoze, S. Lupia and W. Ochs, *Eur. Phys. J. C* **5**, 77 (1998).
7. I.M. Dremin and J.W. Gary, *Phys. Lett. B* **B459**, 341 (1999); I.M. Dremin and J.W. Gary, hep-ph/0004215; A. Capella et al., *Phys. Rev. D* **61**, 074009 (2000).
8. I.M. Dremin and J. Tran Thanh Van, hep-ph/0008054.
9. CLEO Collab., M.S. Alam et al., *Phys. Rev. D* **46**, 4822 (1992); CLEO Collab., M.S. Alam et al., *Phys. Rev. D* **56**, 17 (1997).
10. OPAL Collab., G. Abbiendi et al., CERN-EP-2000-070.
11. DELPHI Collab., P. Abreu et al., *Phys. Lett. B* **449**, 383 (1999); DELPHI Collab., CERN-OPEN-2000-134.
12. ZEUS Collab., Contribution #906 to ICHEP 2000.
13. OPAL Collab., P.D. Acton et al., *Z. Phys. C* **58**, 387 (1993).
14. C. Peterson and T.F. Walsh, *Phys. Lett. B* **B91**, 455 (1980).
15. DELPHI Collab., P. Abreu et al., *Phys. Lett. B* **B401**, 118 (1997); OPAL Collab., K. Ackerstaff et al., *Eur. Phys. J. C* **8**, 241 (1999); DELPHI Collab., P. Abreu et al., CERN-EP-2000-007.
16. L3 Collab., M. Acciarri et al., *Phys. Lett. B* **407**, 389 (1997).
17. L3 Collab., M. Acciarri et al., *Phys. Lett. B* **371**, 126 (1996).
18. ALEPH Collab., R. Barate et al., CERN-EP/99-105.
19. Yu. Dokshitzer et al., Basics of perturbative QCD, Editions Frontières (1991).